

Quantum statistics of the collective excitations of an atomic ensemble inside a cavity

Jin-Feng Huang (黄金凤),¹ Qing Ai (艾清),¹ Yuangang Deng (邓元刚),² C. P. Sun (孙昌璞),¹ and Franco Nori (野理)^{3,4}

¹*Institute of Theoretical Physics, Chinese Academy of Sciences, Beijing 100190, China*

²*Department of Physics, Henan Normal University, Xinxiang 453007, China*

³*Advanced Science Institute, RIKEN, Wako-shi, Saitama 351-0198 Japan*

⁴*Department of Physics, University of Michigan, Ann Arbor, Michigan 48109-1040, USA*

(Received 20 October 2011; published 2 February 2012)

We study the quantum statistical properties of the collective excitations of an atomic ensemble inside a high-finesse cavity. In the large-detuning regime, it is found that the virtual photon exchange can induce a long-range interaction between atoms, which results in correlated excitations. In particular, the atomic blockade phenomenon occurs when the induced long-range interaction effectively suppresses the double atomic excitation, when the average photon number takes certain values, which makes the two nearest energy levels degenerate. We also show that quantum phase transitions occur in the indirectly interacting atomic ensemble when the average photon number reaches several critical points. In this sense, the quantum statistical properties of the collective excitations are very sensitive to the change of the average photon number. Our model exhibits quantum phase transitions similar to the ones in the Lipkin-Meshkov-Glick model. Our proposal could be implemented in a variety of systems including cavity quantum electrodynamics (QED), Bose-Einstein condensates, and circuit QED.

DOI: [10.1103/PhysRevA.85.023801](https://doi.org/10.1103/PhysRevA.85.023801)

PACS number(s): 42.50.Nn, 42.50.Dv, 73.43.Nq

I. INTRODUCTION

In quantum optics, photon statistics reflect the essential properties of the electromagnetic field [1]. Importantly, correlated photon counting by the second-order correlation function can characterize the very quantum nature of light, such as bunching and antibunching effects [2], as well as the photon blockade [3,4], which is also referred to as optical state truncation [5]. The quantum statistical approach for photon counting [6] is also applicable to other massive and massless bosons [7]. The collective excitations of an atomic ensemble could be regarded as an operational quantum memory [8,9] and the ensemble behaves as a boson in the large N limit with low excitations [10]. Therefore, it is expected that the quantum statistical approach can also work well for atomic collective excitations. Moreover, the quantum correlations of these excitations can also be responsible for double-excitation effects, such as the Rydberg blockade, where double excitation is strongly suppressed by the dipole-dipole interaction between highly excited Rydberg atoms [11–13].

The atomic blockade is similar to the Coulomb blockade, a typical mesoscopic phenomenon where a single electron prevents an electric current from crossing some confined nanostructure [14–17]. Similar blockade effects have been predicted and also observed in quantum optical system for photons [3,4] and cold atoms [11–13,18]. Recently, phonon blockade has also been studied [19]. The blockade effect, whereby a single particle prevents the flow [3,4,14–16,18] or excitation of many particles, provides a mechanism for the precise manipulation of quantum states of microscopic quantum objects at the level of a single particle. In this sense, it is essential for the implementation of single-particle-based quantum devices. The photon blockade effect may have applications in single-photon sources, needed for the physical implementation of quantum cryptography protocols [20].

In this paper we consider quantum correlation effects for an atomic system. One of the correlation effects studied is

the Rydberg blockade effect. We consider a similar atomic blockade effect using an indirect-interaction coupling, which is induced by some confined photons in a cavity rather than by dipole-dipole interactions between atoms, as in the Rydberg blockade. Physical properties of atomic ensembles can also be quantified via spin squeezing [21].

Specifically, we study the case where an ensemble of two-level atoms are coupled to a cavity field with a large detuning frequency. The photons in the cavity can induce excitation hopping among atoms, which form a collective excited state described by the number of excited atoms. We will consider the case where the number of excited atoms is similar to the difference between the numbers of excited atoms and unexcited atoms. Furthermore, the variation of half of this difference equals the variation of the number of excited atoms.

Similar to the generic Coulomb interaction for the Rydberg blockade [11–13], the induced interaction by cavity photons is also a long-range interaction and results in inhomogeneous energy-level spacings. More specifically, the structure of the energy levels depends on the average photon number. We find that there will be two degenerate energy levels at an integral multiple of $1/2$ for the average photon number. If the average photon number slightly deviates from an odd multiple of $1/2$, these two degenerate levels will become nearly degenerate but far away from other energy levels. Hence, it is difficult for the atomic ensemble to transit from the nearly degenerate levels to other levels. This shows that the double excitation requires higher energy, which is off-resonant to two single excitations. Therefore, the atomic blockade effect could occur. If we further change the average photon number, the pair of nearly degenerate energy levels shifts far away from each other, but one of them could end up closer to a neighboring energy level which was far away from this pair before changing the average photon number. Thus, the occurrence of atomic blockade can be controlled by the average photon number in the cavity.

Meanwhile, a quantum phase transition (QPT) [22–24] occurs when the average photon number is a half-integer, for negative detuning (the difference between the atomic energy-level spacing and the frequency of the cavity field). This is partially due to the energy-level crossing under the above conditions. The ground state changes drastically around the critical points characterized by the average photon number. This QPT behavior is similar to that of the Lipkin-Meshkov-Glick (LMG) model [25], which was studied in the quantum-information-process context in, for example, Ref. [26]. In this sense, we can regard our system as a modification of the LMG model. However, the critical points in our system are average-photon-number dependent. This provides a controllable way to manipulate the system between different phases.

To characterize various correlation phenomena of the atomic collective excitation, such as the atomic blockade and sensitivity of the QPT [27–31], we introduce a generalized second-order coherence function by replacing the annihilation (creation) a (a^\dagger) operator of photons in the usual second-order coherence function of photons with the lowering (raising) J_- (J_+) operator of the collective atomic excitations. We prove that the antibunching effect occurs near odd multiples of $1/2$ for the photon number, which implies that the double atomic excitation is suppressed. We also find significantly different behaviors on either side of the critical points.

This paper is organized as follows. In Sec. II, we describe the system based on the Dicke model [29,32]. The effective Hamiltonian is given in terms of the collective excitation of the atomic ensemble, and the ground state is analyzed for different APNs. In Sec. III we then coherently drive the atomic ensemble and derive the effective Hamiltonian near two critical points $n_a^c = 1/2$ and $n_a^c = j - 1/2$. In Sec. IV, we introduce the generalized second-order coherence function and calculate the statistical properties of the excitations of the atomic ensemble in the cases with and without dissipation. We discuss the atomic blockade effect and sensitivity of the QPT to the photon number in Secs. V and VI, respectively. Finally, we present our conclusions in Sec. VII. The explicit form of the parameters used in Secs. IV and VI are given in the Appendix.

II. QUANTUM CRITICALITY OF AN ATOMIC ENSEMBLE STRONGLY COUPLED TO A CAVITY FIELD

A. Model and Hamiltonian

As shown in Fig. 1, the system we consider consists of an ensemble of atoms confined to a single-mode cavity of frequency ω . The cavity field is described by the annihilation (creation) operator a (a^\dagger). This model can be implemented in a variety of systems including cavity QED [33], Bose-Einstein condensates [34], and circuit QED [35].

Our model is described by the Dicke Hamiltonian [29,32,35–40] (hereafter, we take $\hbar = 1$),

$$H_1 = \omega a^\dagger a + \frac{\omega_A}{2} \sum_{\ell=1}^N \sigma_z^{(\ell)} + \frac{g_0}{\sqrt{N}} \sum_{\ell=1}^N (a^\dagger \sigma_-^{(\ell)} + a \sigma_+^{(\ell)}), \quad (1)$$

under the rotating-wave approximation. Here, we use the Pauli matrices $\sigma_z^{(j)} = |e\rangle_{jj}\langle e| - |g\rangle_{jj}\langle g|$, $\sigma_+^{(j)} = |e\rangle_{jj}\langle g|$, and $\sigma_-^{(j)} = |g\rangle_{jj}\langle e|$ to describe the atomic transition of the j th

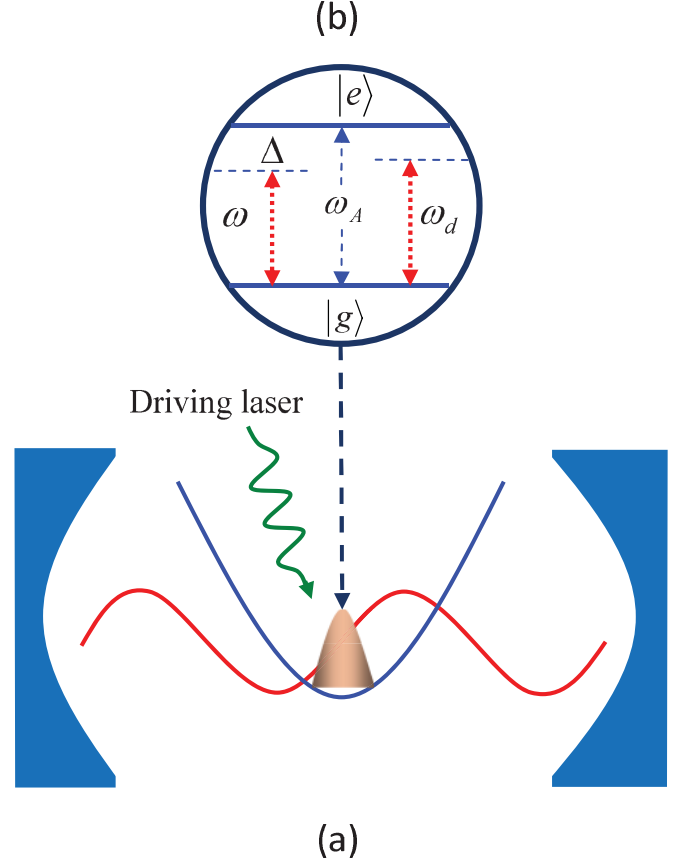


FIG. 1. (Color online) (a) Schematic of a cavity field of frequency ω coupled to an atomic gas consisting of N two-level atoms with energy-level spacing ω_A . A driving field of strength Ω_d and frequency ω_d is applied to the atoms. (b) The coupling diagram of one of the two-level atoms in the cavity. Here, Δ is the detuning between the atomic level spacing ω_A and the cavity field frequency ω , namely, $\Delta \equiv \omega_A - \omega$, and ω_d is the frequency of the drive.

atom with energy-level spacing ω_A , where $|e\rangle_j$ and $|g\rangle_j$ are the excited and ground states of the j th atom, respectively.

For an atomic gas with size smaller than the wavelength [29,31], we assume that all the atoms are located near the origin and interact with the cavity field at the homogeneous coupling rate g_0/\sqrt{N} . Here, the factor \sqrt{N} in the denominator of the coupling strength originates from the fact that the coupling strength is inversely proportional to the square root of the volume of the cavity field $1/\sqrt{V}$. The volume V is approximately equal to the total volume occupied by the atoms, which is N times the volume of a single atom. Hence we can write the factor \sqrt{N} explicitly in the coupling strength.

We would like to point out that, the superradiant phase transition based on the Dicke model in a real atomic system does not exist due to the inclusion of electromagnetic vector potential A^2 term [29,37,41,42]. However, the following arguments about QPT are based on the LMG model [25], which will be derived from the above Dicke model, even including the A^2 term. The similar A^2 term (V^2 term) in circuit QED system will not influence the Hamiltonian significantly, except for just a little shift of the critical point [43].

The atoms we consider are largely detuned from the frequency ω of the cavity field; namely, the detuning Δ

($\equiv \omega_A - \omega$) is much larger than the corresponding coupling strength g_0/\sqrt{N} , that is, $|\Delta| \gg |g_0/\sqrt{N}|$. In this case, one can use the Fröhlich-Nakajima transformation [44,45] (or adiabatic elimination method), to obtain the effective Hamiltonian,

$$H_1 = \omega a^\dagger a + \frac{1}{2}(\omega_A + W) \sum_{\ell=1}^N \sigma_z^{(\ell)} + W \sum_{\ell=1}^N a^\dagger a \sigma_z^{(\ell)} + \frac{1}{2}W \sum_{\ell_1, \ell_2=1}^N (\sigma_+^{(\ell_1)} \sigma_-^{(\ell_2)} + \sigma_-^{(\ell_1)} \sigma_+^{(\ell_2)}), \quad (2)$$

where $W = g_0^2/(N\Delta)$ is the strength of the effective interaction among the atoms, which is induced by the virtual photon exchanges. The form of the Hamiltonian is very similar to the dipole-dipole interaction of atoms in free space. We note that the Fröhlich-Nakajima transformation is equivalent to the approach based on the adiabatical elimination and some perturbation theories [46]. Furthermore, the photon number $a^\dagger a$ becomes a conserved number.

B. Symmetric Hilbert space and the LMG model

We now describe the Hilbert space of the symmetric excitation. The Hilbert space of N two-level atoms is spanned by 2^N basis vectors $\{|g_l\rangle, |e_l\rangle\}$ with $l = 1, 2, \dots, N$. In the present case, all the atoms have identical transition frequencies and coupling constants with the cavity field. Here, we consider the symmetric collective excitation subspace $V^{[1]}$ of dimension $(N+1)$. We now introduce the collective operators,

$$J_\pm = \sum_{\ell=1}^N \sigma_\pm^{(\ell)}, \quad J_z = \frac{1}{2} \sum_{\ell=1}^N \sigma_z^{(\ell)}, \quad (3)$$

which obey the following angular momentum commutation relations,

$$[J_z, J_\pm] = \pm J_\pm, \quad [J_+, J_-] = 2J_z. \quad (4)$$

Furthermore, we define the Dicke basis vectors $|j, m\rangle$ ($j = N/2$, $m = -j, -j+1, \dots, j-1, j$), which satisfy $J^2|j, m\rangle = j(j+1)|j, m\rangle$, and $J_z|j, m\rangle = m|j, m\rangle$. One can conclude straightforwardly from Eq. (3) that the magnetic quantum number m equals the half difference between the numbers of excited atoms and the ground-state atoms. In terms of the Dicke states, the symmetric excitation subspace, $V^{[1]}$, is

$$|j, m\rangle = \mathcal{N}_m J_+^{j+m} |j, -j\rangle = \mathcal{N}_m \left[\sum_{\ell=1}^N \sigma_+^{(\ell)} \right]^{j+m} |G\rangle, \quad (5)$$

where $\mathcal{N}_m = \sqrt{(j-m)!/[(2j)!(j+m)!]}$ and $|G\rangle = |g_1, g_2, \dots, g_N\rangle$.

According to Eq. (3), we can find

$$J_\pm |j, m\rangle = \sum_{\ell=1}^N \sigma_\pm^{(\ell)} |j, m\rangle = \sqrt{(j \pm m + 1)(j \mp m)} |j, m \pm 1\rangle. \quad (6)$$

It follows from Eq. (6) that the ladder operators J_\pm describe the action of pumping one more (J_+) or less (J_-) atom from

the ground state $|g\rangle$ to the excited state $|e\rangle$. Accordingly, the magnetic quantum number m increases or decreases by one. Therefore, when the ladder operator J_+ acts on the collective-excitation state s ($0 \leq s \leq N$) times, there will be s atoms being excited, and the magnetic quantum number m will increase by s accordingly: namely $|j, m\rangle \rightarrow |j, m+s\rangle$, which is implied in Eq. (5). As for the ladder operator J_- , the effect is inverse. Therefore, the variance of the magnetic quantum number m represents the variance of the atomic-collective-excitation number.

In terms of the above collective operators, the Hamiltonian (2) can be rewritten as

$$H_1 = \omega a^\dagger a + (\omega_A + W)J_z + 2Wa^\dagger a J_z + \frac{W}{2}(J_+ J_- + J_- J_+). \quad (7)$$

In the interaction picture defined with respect to the free Hamiltonian, $H_{\text{free}} = \omega a^\dagger a + (\omega_A + W)J_z$, the Hamiltonian reads

$$H_1^{(I)} = \varepsilon(\hat{n}_a)J_z + \frac{W}{2}(J_+ J_- + J_- J_+), \quad (8)$$

where $\hat{n}_a = a^\dagger a$ and $\varepsilon(\hat{n}_a) = 2W\hat{n}_a$. The effective Hamiltonian (8) is photon-number dependent. This is a special case of the LMG model [25] with $V = 0$. The LMG model can also be implemented using superconducting circuits [47,48]. Through the relations $(J_+ J_- + J_- J_+)/2 = J_x^2 + J_y^2$, the Hamiltonian can be expressed as

$$H_1^{(I)} = -W[(J_z - \hat{n}_a)^2 - \hat{n}_a^2 - J^2]. \quad (9)$$

As is well known, the LMG model possesses a critical point, at which a QPT occurs. On either side of the critical point, the number of excited atoms of the ground states are different; thus the ground states are essentially different [28,49,50]. In our system, a similar critical point also exists. To see this effect explicitly, we calculate the ground state for the above Hamiltonian in the next section.

The last two terms of Eq. (8) describe the interaction among atoms induced by photons in the cavity. This interaction between atoms is intrinsically caused by the hopping of photons between different atoms. And the hopping of photons induces a second-order indirect interaction among atoms. On account of this interaction, the system shows an obvious nonlinearity with respect to the excitation number, as shown by Eq. (9).

C. Quantum phase transition behavior of the ground state

We now analyze the discontinuous change of the ground-state symmetry when varying the photon number. For a given Fock state of the field, $\varepsilon(\hat{n}_a)$ is a definite c number. For a general photon state $|\psi\rangle$ we replace $\varepsilon(\hat{n}_a)$ by its mean value such as $\varepsilon(\langle \hat{n}_a \rangle)$ [or $\varepsilon(\langle n_a \rangle)$] when our studies only concern the atomic ensemble. According to Eq. (9), the eigenstates of the system are the common eigenstates of $\{J^2, J_z\}$: $\{|j, m\rangle; m = -j, -j+1, \dots, j-1, j\}$, for $j = N/2$, that is,

$$H_1^{(I)}|j, m\rangle|\psi\rangle = E_m^{(0)}|j, m\rangle|\psi\rangle, \quad (10)$$

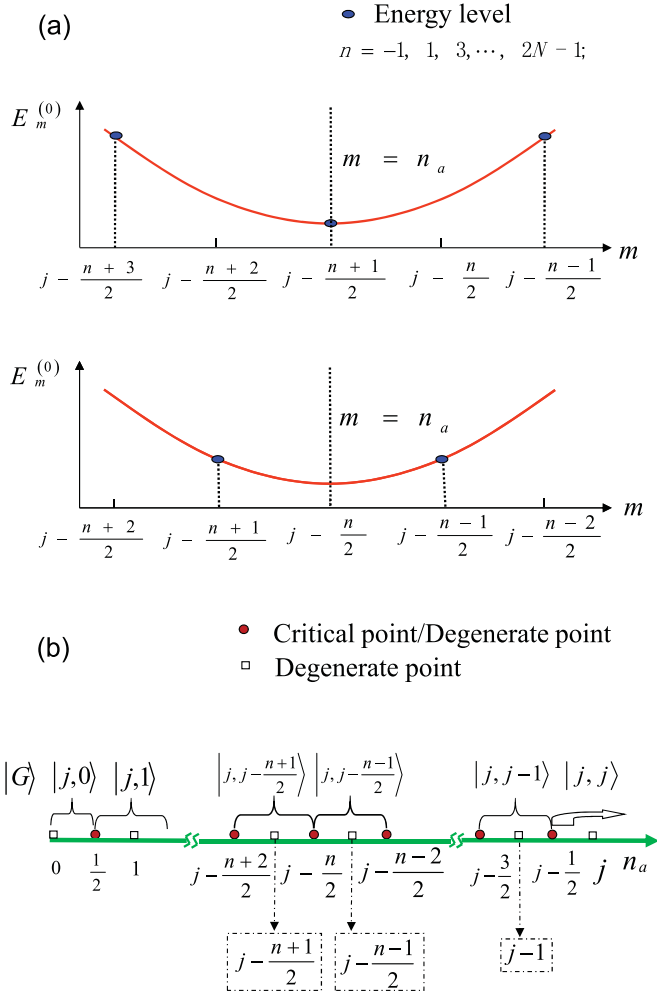


FIG. 2. (Color online) Diagram of the ground state of atoms consisting of N two-level atoms controlled by the cavity photon number when $\Delta < 0$. (a) Diagram of the energy levels versus the magnetic quantum number m . The upper figure in (a) shows the ground state located at $m = n_a = j - (n + 1)/2$; the lower figure in (a) shows the two degenerate ground states located at $m = j - (n + 1)/2$, $j - (n - 1)/2$, respectively, while $n_a = j - n/2$. (b) Diagram of the ground states corresponding to different average photon numbers in the cavity.

with eigenenergies,

$$E_m^{(0)} = -W[(m - n_a)^2 - n_a^2 - j(j + 1)] \equiv \omega_m. \quad (11)$$

Clearly, the ground state is photon-number dependent, that is,

$$|G\rangle = \begin{cases} |j, [n_a]\rangle, & 0 \leq n_a \leq j - \frac{1}{2}, & \Delta < 0, \\ |j, j\rangle, & n_a \geq j - \frac{1}{2}, & \Delta < 0, \\ |j, -j\rangle \text{ or } |j, j\rangle, & n_a = 0, & \Delta > 0, \\ |j, -j\rangle, & n_a > 0, & \Delta > 0, \end{cases} \quad (12)$$

where $[n]$ denotes the (half) integer nearest to n . This fact means that the ground-state symmetry changes suddenly when the photon number is varied from one domain to another.

In the following discussions, we restrict the analysis to the negative detuning $\Delta < 0$. As shown in Fig. 2, when the

value of the photon number n_a is varied in the domain of $0 \leq n_a \leq j - 1/2$, the atoms will experience different ground states, which implies that QPTs occur.

There are energy-level crossings at $n_a^c = j - n/2$, ($n = 1, 3, 5, \dots, 2j - 1$). In the domain $j - (n + 2)/2 < n_a < j - (n + 1)/2$, the ground state of the system is $|G\rangle = |j, j - (n + 1)/2\rangle$, where as in the next domain $j - n/2 < n_a < j - (n - 2)/2$, the ground state of the system is $|G\rangle = |j, j - (n - 1)/2\rangle$. If n_a increases from $j - (n + 2)/2$ to $j - (n - 2)/2$, the energy level of the excited state crosses the energy level of the ground state at $n_a^c = j - n/2$. At the level crossing, the excited state $|j, j - (n - 1)/2\rangle$ and the ground state $|j, j - (n + 1)/2\rangle$ are degenerate. On the right side of this critical point n_a^c , the original excited state $|j, j - (n - 1)/2\rangle$ in the domain of $j - (n + 2)/2 < n_a < j - n/2$ will become a new ground state for the system in the domain of $j - n/2 < n_a < j - (n - 2)/2$, which implies that a QPT occurs. In this sense, we can use the average photon number n_a to control the occurrence of the quantum phase transition. At the critical point $n_a^c = j - n/2$, both $|j, j - (n + 1)/2\rangle$ and $|j, j - (n - 1)/2\rangle$ are the ground states. Moreover, at this point, the ground state is highly degenerate, thus the system is in a symmetric phase.

In other domains, namely, when $\Delta < 0$ and $n_a > j - 1/2$, or, $\Delta > 0$, the ground state is $|j, j\rangle$ or $|j, -j\rangle$. In these cases, all the atoms are fully polarized. As all the two-level atoms can be considered as quasispins, the system is ferromagnetic in this domain, and the rotational symmetry is broken. Thus the system is in a symmetry-broken phase. Notice that in the left vicinity of the critical points n_a^c , under the condition $\Delta < 0$, the ground state is $|j, m = [n_a]\rangle$ and possesses one less atomic excitation than that in the first excited state $|j, [n_a] + 1\rangle$. It is clear that $|j, [n_a]\rangle$ and $|j, [n_a] + 1\rangle$ are nearly degenerate, but their energies are much less than that of $|j, [n_a] + 2\rangle$. Thus, there exists an energy gap that makes exciting two more atoms difficult, but easy for exciting one more atom. We call this effect ‘‘atomic blockade.’’

III. DRIVEN ATOMIC ENSEMBLE

As there exists a level crossing for the photon-dressed atomic ensemble at $n_a = n_a^c$, we apply a weak classical driving to the atomic ensemble. The interaction is described by the Hamiltonian,

$$H_2 = \Omega \sum_{\ell=1}^N (\sigma_-^{(\ell)} e^{i\omega_d t} + \sigma_+^{(\ell)} e^{-i\omega_d t}), \quad (13)$$

where Ω is the Rabi frequency and ω_d is the driving frequency of the drive. The total Hamiltonian $H = H_1 + H_2$ becomes

$$H^{(R)} = H_1^{(I)} + (\omega_A + W - \omega_d)J_z + \Omega(J_- + J_+) \quad (14)$$

in a rotating frame with rotation $\exp[i(\omega_d J_z + \omega a^\dagger a)t]$. In this driven case, the photon number $a^\dagger a$ still is a conserved number. Therefore the photon number does not change in the dynamical evolution even though we apply a classical driving field. As a result, we can treat the photon number as an independent external parameter, which is decoupled from the atomic dynamics. We tune the frequency ω_d to satisfy the resonance condition $\omega_A + W - \omega_d = 0$. Then the simplified

Hamiltonian is $H^{(R)} = H_1^{(I)} + H'$ with $H' = \Omega(J_- + J_+)$. When the optical field is prepared in a coherent state $|\alpha\rangle$, the Hamiltonian, after this average $\hat{n}_a \rightarrow n_a = \langle \hat{n}_a \rangle$, reads

$$H^{(R)} = -W[(J_z - n_a)^2 - n_a^2 - J^2] + \Omega(J_- + J_+), \quad (15)$$

where $\langle \hat{n}_a \rangle = |\alpha|^2$, for $n_a \equiv 1/2 + \delta$. Here δ is the deviation from the degenerate (critical) point. To see if the atomic blockade effect occurs, we express the above-averaged Hamiltonian in the angular momentum basis as

$$H^{(R)} = \sum_{m=-j}^j \omega_m |j, m\rangle \langle j, m| + \sum_{m=-j}^{j-1} \Omega_{m+1} (|j, m+1\rangle \langle j, m| + \text{H.c.}), \quad (16)$$

where $\Omega_m = \Omega\sqrt{(j-m+1)(j+m)}$. We can then more readily observe the transition from $|j, m\rangle$ to $|j, m+2\rangle$ by exciting two more atoms around the critical point n_a^c .

A. Reduced dynamics on the subspace with $m = 0, 1$

When the photon number n_a is in the vicinity of $1/2$, the nearly degenerate energy levels $m = 0, 1$ ($|j, 0\rangle$ and $|j, 1\rangle$) will be strongly coupled with each other as a result of the driving, but weakly coupled with other energy levels. Then the two energy levels ($m = 0, 1$) form a relatively stable subsystem. Hence we can treat the transitions from the subsystem to other levels by a perturbative approach. In terms of the states with definite quantum number m , the Hamiltonian $H^{(R)} = H_0 + H_I$ can be decomposed in two parts, the nonperturbative Hamiltonian,

$$H_0 = \omega_0 |j, 0\rangle \langle j, 0| + \omega_1 |j, 1\rangle \langle j, 1| + \Omega\sqrt{j(j+1)} |j, 1\rangle \langle j, 0| + \text{H.c.}, \quad (17)$$

and the perturbation,

$$H_I = \Omega_2 |j, 2\rangle \langle j, 1| + \Omega_0 |j, 0\rangle \langle j, -1| + \sum_{m=-j, m \neq 0, 1}^j \omega_m |j, m\rangle \langle j, m| + \sum_{m=-j, m \neq -1, 0, 1}^{j-1} \Omega_{m+1} |j, m+1\rangle \langle j, m| + \text{H.c.} \quad (18)$$

To see clearly if the atomic blockade effect occurs, namely, if it is difficult to excite two more atomic excitations, we need to find the transition amplitude for the system initially prepared in the subspace spanned by $|j, 0\rangle$ and $|j, 1\rangle$ to the doubly excited state $|j, 2\rangle$ around the critical point $n_a = 1/2$. To make $|j, 0\rangle$ and $|j, 1\rangle$ nearly degenerate, we restrict $0 < n_a < 1$. We note that we can also choose any other pair of nearly degenerate states around the corresponding critical point which makes the pair nearly degenerate. We first diagonalize the nonperturbative Hamiltonian (17) as

$$H_0 = \lambda_0 |\lambda_0\rangle \langle \lambda_0| + \lambda_1 |\lambda_1\rangle \langle \lambda_1|. \quad (19)$$

The two eigenstates are

$$|\lambda_r\rangle = A_r^{-1} [\xi_r |j, 0\rangle + |j, 1\rangle], \quad r = 0, 1, \quad (20)$$

with corresponding eigenenergies,

$$\lambda_r = jW + j^2W + W\delta + (-1)^{r+1}p, \quad (21)$$

where $A_r = \sqrt{|\xi_r|^2 + 1}$ are normalization constants with

$$\xi_r = -\frac{W\delta + (-1)^r p}{\Omega\sqrt{j(j+1)}}, \quad (22)$$

and

$$p \equiv \sqrt{W^2\delta^2 + j^2\Omega^2 + j^2\Omega^2}. \quad (23)$$

We note that $\langle j, m | \lambda_r \rangle = 0$ for $m \neq 0, 1$. Therefore, $|\lambda_0\rangle$, $|\lambda_1\rangle$ and $|j, m\rangle$ ($m \neq 0, 1$) form a complete basis of the Hilbert space for a given j . In this basis, H_I can be expressed as

$$H_I = \Omega_2 [\eta_1 |j, 2\rangle \langle \lambda_0| + \eta_2 |j, 2\rangle \langle \lambda_1|] + \Omega_0 [\eta_3 |\lambda_0\rangle \langle j, -1| + \eta_4 |\lambda_1\rangle \langle j, -1|] + \sum_{m=-j, m \neq 0, 1}^j \omega_m |j, m\rangle \langle j, m| + \sum_{m=-j, m \neq -1, 0, 1}^{j-1} \Omega_{m+1} |j, m+1\rangle \langle j, m| + \text{H.c.}, \quad (24)$$

where

$$\eta_1 = \frac{\xi_1 A_0}{\xi_1 - \xi_0}, \quad \eta_2 = -\frac{\xi_0 A_1}{\xi_1 - \xi_0}, \quad (25)$$

$$\eta_3 = \frac{A_0}{\xi_0 - \xi_1}, \quad \eta_4 = -\frac{A_1}{\xi_0 - \xi_1},$$

which satisfy $|\eta_1|^2 + |\eta_2|^2 = 1$ and $|\eta_3|^2 + |\eta_4|^2 = 1$. It follows from Eq. (24) that the transition between $|\lambda_0\rangle$ and $|\lambda_1\rangle$ is inhibited, which is shown in Fig. 3. In order to calculate the correlation function $g^{(2)}$ with the perturbed Hamiltonian, we move to the interaction picture by choosing

$$H'_0 = \lambda_0 |\lambda_0\rangle \langle \lambda_0| + \lambda_1 |\lambda_1\rangle \langle \lambda_1| + \sum_{m=-j, m \neq 0, 1}^j \omega_m |j, m\rangle \langle j, m| \quad (26)$$

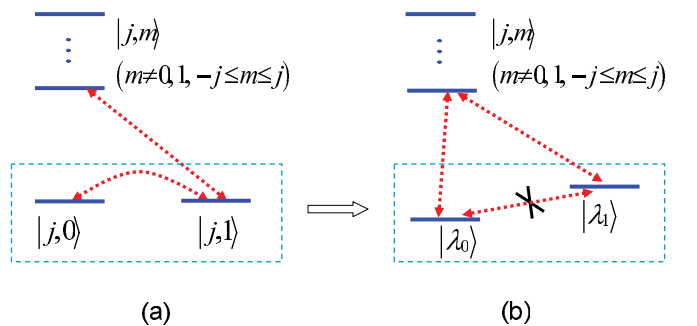


FIG. 3. (Color online) Energy-level diagram of the $m = 0, 1$ subsystem of the driven atomic ensemble. (a) The two nearly degenerate energy levels $|j, 0\rangle$ and $|j, 1\rangle$ are strongly coupled with each other, when the average photon number in the cavity is $n_a \approx 1/2$, but weakly coupled with other energy levels. (b) The effective subsystem spanned by $|\lambda_0\rangle$ and $|\lambda_1\rangle$ when using the perturbation approach.

as the free Hamiltonian. In the interaction picture, the Hamiltonian $H^{(R)} = H_0' + H_I'$, where

$$H_I' = \sum_{m=-j, m \neq 0}^j \Omega_{m+1} |j, m+1\rangle \langle j, m| + \text{H.c.} \quad (27)$$

becomes

$$\begin{aligned} V_I(t) = & \Omega_2 |j, 2\rangle (\eta_1 \langle \lambda_0 | e^{i\Delta_{2,0}t} + \eta_2 \langle \lambda_1 | e^{i\Delta_{2,1}t}) \\ & + \Omega_0 (\eta_3 \langle \lambda_0 | e^{-i\Delta_{-1,0}t} + \eta_4 \langle \lambda_1 | e^{-i\Delta_{-1,1}t}) \langle -1, j | \\ & + \sum_{m=-j, m \neq -1, 0, 1}^{j-1} \Omega_{m+1} |j, m+1\rangle \langle m, j | e^{i\omega_{m+1, m}t} + \text{H.c.}, \end{aligned} \quad (28)$$

which is time dependent. Here, we have defined

$$\Delta_{m', r} \equiv \omega_{m'} - \lambda_r, \quad \omega_{m, l} \equiv \omega_m - \omega_l, \quad (29)$$

where $m' \neq 0, 1$, $r = 0, 1$, and $\Delta_{m', r}$ is the energy difference between the diagonalized almost-degenerate energy levels labeled by $|\lambda_r\rangle$ ($r = 0, 1$) and the other energy levels labeled by $|j, m\rangle$ ($m \neq 0, 1$).

B. Reduced dynamics on the subspace with $m = j - 1, j$

Here we consider the effect of the QPT on the higher-order quantum coherence around the critical point $n_a = j - 1/2$. Similar to the previous section, it can be seen that the states $|j, j - 1\rangle$ and $|j, j\rangle$ form a relative stable subsystem. We can also treat the transitions from the subsystem ($m = j - 1, j$) to other energy levels by using a perturbative method. To this end we diagonalize the Hamiltonian in the subspace spanned by the two nearly degenerate energy levels $|j, j - 1\rangle$ and $|j, j\rangle$. It follows from Eq. (16) that, the nonperturbative Hamiltonian is

$$\begin{aligned} H_0^c = & \omega_j |j, j\rangle \langle j, j| + \omega_{j-1} |j, j-1\rangle \langle j, j-1| \\ & + \Omega_j |j, j\rangle \langle j, j-1| + \text{H.c.} \\ \equiv & \lambda_0^c |\lambda_0^c\rangle \langle \lambda_0^c| + \lambda_1^c |\lambda_1^c\rangle \langle \lambda_1^c|, \end{aligned} \quad (30)$$

with the eigenenergies,

$$\begin{aligned} \lambda_r^c = & 2^{-1} [-1 - 2n_a + 4j(1 + n_a)]W \\ & + 2^{-1} (-1)^{r+1} p^c, \quad r = 0, 1, \end{aligned} \quad (31)$$

and eigenvectors,

$$|\lambda_r^c\rangle = (A_r^c)^{-1} [\xi_r^c |j, j-1\rangle + |j, j\rangle], \quad r = 0, 1, \quad (32)$$

where $A_r^c = \sqrt{|\xi_r^c|^2 + 1}$ ($r = 0, 1$) are normalization constants with

$$\xi_r^c = [2\Omega\sqrt{2j}]^{-1} [(-1 + 2j - 2n_a)W + (-1)^{r+1} p^c], \quad (33)$$

and

$$p^c \equiv \sqrt{(1 - 2j + 2n_a)^2 W^2 + 8j\Omega^2}. \quad (34)$$

Similar to the above Sec. III A, we also note that $\langle j, m | \lambda_r^c \rangle = 0$ for $m \neq j - 1, j$. Therefore, $|\lambda_0^c\rangle$, $|\lambda_1^c\rangle$ and $|j, m\rangle$ ($m \neq j - 1, j$) form a complete basis of the Hilbert space for a given j . In terms of $|\lambda_0^c\rangle$ and $|\lambda_1^c\rangle$, the residual terms of the Hamiltonian

(16) $H_I^c = H^{(R)} - H_0^c$ read as

$$\begin{aligned} H_I^c = & \Omega_{j-1} [(\eta_3^c |\lambda_0^c\rangle + \eta_4^c |\lambda_1^c\rangle) \langle j, j-2| + \text{H.c.}] \\ & + \sum_{m=-j}^{j-2} \omega_m |j, m\rangle \langle j, m| \\ & + \sum_{m=-j}^{j-3} \Omega_{m+1} (|j, m+1\rangle \langle j, m| + \text{H.c.}), \end{aligned} \quad (35)$$

where we used the expressions,

$$|j, j\rangle = \eta_1^c |\lambda_0^c\rangle + \eta_2^c |\lambda_1^c\rangle, \quad |j, j-1\rangle = \eta_3^c |\lambda_0^c\rangle + \eta_4^c |\lambda_1^c\rangle, \quad (36)$$

with coefficients defined by

$$\begin{aligned} \eta_1^c = & \frac{\xi_1^c A_0^c}{\xi_1^c - \xi_0^c}, & \eta_2^c = & -\frac{\xi_0^c A_1^c}{\xi_1^c - \xi_0^c}, \\ \eta_3^c = & \frac{A_0^c}{\xi_0^c - \xi_1^c}, & \eta_4^c = & -\frac{A_1^c}{\xi_0^c - \xi_1^c}, \end{aligned} \quad (37)$$

which satisfy $|\eta_1^c|^2 + |\eta_2^c|^2 = 1$, $|\eta_3^c|^2 + |\eta_4^c|^2 = 1$. It follows from Eq. (35) that there is no transition between $|\lambda_0^c\rangle$ and $|\lambda_1^c\rangle$, which is shown in Fig. 4. In order to change to the interaction picture, we choose the diagonalized terms,

$$H_0^c = \lambda_0^c |\lambda_0^c\rangle \langle \lambda_0^c| + \lambda_1^c |\lambda_1^c\rangle \langle \lambda_1^c| + \sum_{m=-j}^{j-2} \omega_m |j, m\rangle \langle j, m|, \quad (38)$$

as the free Hamiltonian, and the corresponding interaction Hamiltonian,

$$H_I^c = \sum_{m=-j}^{j-2} \Omega_{m+1} (|j, m+1\rangle \langle j, m| + \text{H.c.}). \quad (39)$$

Finally, we obtain the interaction Hamiltonian,

$$\begin{aligned} V_I^c(t) = & \Omega_{j-1} (\eta_3^c |\lambda_0^c\rangle e^{-i\Delta_{j-2,0}^c t} + \eta_4^c |\lambda_1^c\rangle e^{-i\Delta_{j-2,1}^c t}) \langle j, j-2| \\ & + \sum_{m=-j}^{j-3} \Omega_{m+1} |j, m+1\rangle \langle j, m| e^{i\omega_{m+1, m}t} + \text{H.c.}, \end{aligned} \quad (40)$$

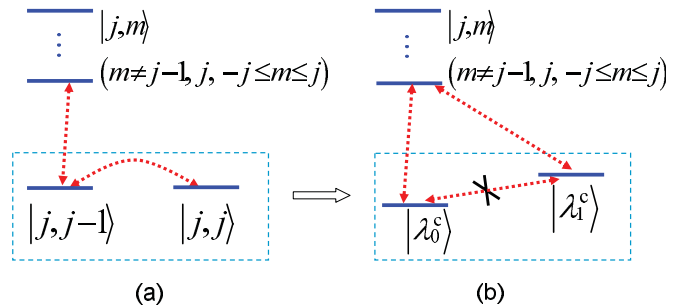


FIG. 4. (Color online) Energy-level diagram of the subsystem composed of $m = j - 1, j$ of the driven atomic ensemble. (a) The two nearly degenerate energy levels $|j, j - 1\rangle$ and $|j, j\rangle$ are strongly coupled with each other, when the average photon number in the cavity is $n_a \approx j - 1/2$, but weakly coupled with other energy levels. (b) The effective subsystem spanned by $|\lambda_0^c\rangle$ and $|\lambda_1^c\rangle$ by the perturbative approach.

in the interaction picture where

$$\Delta_{m',r}^c \equiv \omega_{m'} - \lambda_r^c, \quad \omega_{m,l} \equiv \omega_m - \omega_l, \quad (41)$$

for $m' \neq j-1, j$, $r = 0, 1$, and $\Delta_{m',r}^c$ is the energy difference between the diagonalized almost degenerate energy levels labeled by $|\lambda_r^c\rangle$ ($r = 0, 1$) and the other energy levels labeled by $|j, m\rangle$ ($m \neq j-1, j$).

Note that Figs. 3 and 4 show transitions between three-level systems, where some of the transitions are turned on and off. Indeed, it is also possible to turn on and off transitions between three energy levels using artificial atoms made of superconducting qubits [51].

IV. STATISTICAL PROPERTIES OF THE ATOMIC EXCITATIONS

Since J_- (J_+) can decrease (increase) a single excitation, their roles are similar to the actions of the annihilation (creation) operator of photons a (a^\dagger) for the usual bosonic system. Using the Holstein-Primakoff transformation [52], the angular momentum operators can be expressed in terms of a single bosonic mode,

$$J_+ = b^\dagger \sqrt{N - b^\dagger b}, \quad J_- = (\sqrt{N - b^\dagger b} b), \quad J_z = b^\dagger b - \frac{N}{2}. \quad (42)$$

The angular momentum operators will become bosonic operators in the limit of large N and low excitations, namely, $\langle b^\dagger b \rangle \ll N$ [29]. Specifically, in this condition, one can expand the square term $\sqrt{N - b^\dagger b}$ on the order of $(b^\dagger b)/N$ and keep to the zeroth order of $b^\dagger b/N$. Then it is straightforward to see that $J_+ \simeq b^\dagger \sqrt{N}$ and $J_- \simeq \sqrt{N} b$ [29]. Then we can define a generalized second-order coherence function,

$$g^{(2)}(\tau, t) = \frac{\langle J_+(t) J_+(t + \tau) J_-(t + \tau) J_-(t) \rangle}{\langle J_+(t) J_-(t) \rangle \langle J_+(t + \tau) J_-(t + \tau) \rangle}, \quad (43)$$

for the symmetric collective excitations of the atomic ensemble, which can be regarded as a normalized correlation function. Please note that this definition is in normal order on the angular momentum operators J_+ and J_- , which satisfy that the average of any analytical function of $J_+ J_-$ in normal order over the ground state $|j, -j\rangle$ equals zero, that is, $\langle j, -j | : f(J_+ J_-) : | j, -j \rangle = 0$. Here j is a conserved quantity. This property satisfies the conventional normal order definition about the bosonic operators $\langle 0 | : f(b^\dagger b) : | 0 \rangle = 0$ in the second coherence function. This coherence function $g^{(2)}(\tau, t)$ is proportional to the joint probability of observing one excited atom at time t and another one at time $t + \tau$. To study the generalized second-order coherence function $g^{(2)}(\tau, t)$ in the stationary state, below we consider it in a unitary evolution case (without dissipation) and also in a dissipation case but at a steady state.

A. The case without dissipation

Firstly, we consider the case where the system is free of dissipation. In this case, $\langle \dots \rangle$ in Eq. (43) for $g^{(2)}(\tau, t)$ denotes

the average of an observable over the initial pure state,

$$|\psi(0)\rangle = \sum_{m=-j}^j c_m |j, m\rangle, \quad (44)$$

where $\sum_{m=-j}^j |c_m|^2 = 1$.

We next calculate the generalized second-order coherence function around the point $\delta = 0$ (i.e., $n_a = 1/2$). Since $U(\tau) = U_0(\tau) U_I(\tau)$, where $U_0(\tau) = \exp(-i H_0' \tau)$ and $U_I(\tau) = T \exp[-i \int_0^\tau V_I(\tau') d\tau']$ are the free evolution and the dynamics due to the interaction, respectively. We note that $U_0^\dagger(\tau) J_+ J_- U_0(\tau) = J_+ J_-$ is useful in the following calculations. Using this result, the generalized second-order coherence function $g^{(2)}(\tau, 0)$ becomes

$$g^{(2)}(\tau, 0) = \frac{\langle \psi'(0) | U_I^\dagger(\tau) J_+ J_- U_I(\tau) | \psi'(0) \rangle}{\langle \psi'(0) | \psi'(0) \rangle \langle \psi(0) | U_I^\dagger(\tau) J_+ J_- U_I(\tau) | \psi(0) \rangle}, \quad (45)$$

where $|\psi'(0)\rangle = J_- |\psi(0)\rangle$. We will calculate analytically the generalized second-order coherence function by applying standard perturbation theory, with $V_I(t)$ as a perturbation. Let us first consider the conditions where the perturbation approach is valid. If we tune the atom-field detuning Δ and the Rabi frequency Ω of the driving field to be suitable and place an appropriate number of atoms in the cavity, we can make the perturbation theory valid, that is, for $m' = 2, -1, r = 0, 1$, and $m \neq -1, 0, 1$ these conditions explicitly are

$$\begin{aligned} \Omega_2 \eta_1 &\ll \Delta_{2,0}, & \Omega_2 \eta_2 &\ll \Delta_{2,1}, \\ \Omega_0 \eta_3 &\ll \Delta_{-1,0}, & \Omega_0 \eta_4 &\ll \Delta_{-1,1}, \\ \Omega_{m+1} &\ll \omega_{m+1,m}. \end{aligned} \quad (46)$$

Under the above conditions, we can treat the time-evolution operator $U_I(\tau)$ perturbatively. When n_a is in the vicinity of the critical point n_a^c (for $m = 0, 1$, $n_a^c = 1/2$), the energy levels of $|\lambda_0\rangle$ and $|\lambda_1\rangle$ are nearly degenerate. The energy differences $\Delta_{i,j}$ and $\omega_{m+1,m}$ ($m \neq -1, 0, 1$) are very large compared with the level spacing between $|\lambda_0\rangle$ and $|\lambda_1\rangle$. Hence, under this constraint, the above conditions (46) can be satisfied by varying the Rabi frequency Ω . Since the state $|j, 0\rangle$ is the ground state when $0 < n_a < 1/2$, then $|j, 1\rangle$ is the state by exciting one more atom. Similarly, $|j, 2\rangle$ has two more excitations than the ground state, and has a much higher energy than that of $|j, 1\rangle$. However, $|j, 1\rangle$ is the ground state when $1/2 < n_a < 1$, yet $|j, 0\rangle$ is an excited state which has one less atomic excitation than the ground state $|j, 1\rangle$. To see if two excitations are suppressed, we choose $c_0 = c_1 = 1/\sqrt{2}$ and $c_m = 0$ (for $m \neq 0, 1$) in the initial state,

$$|\psi(0)\rangle = c_0 |j, 0\rangle + c_1 |j, 1\rangle = \frac{1}{\sqrt{2}} (|j, 0\rangle + |j, 1\rangle). \quad (47)$$

When the average photon number is in the vicinity of $n_a^c = 1/2$, the states $|j, 0\rangle$ and $|j, 1\rangle$ are nearly degenerate. Notice that here the average photon number is in the domain of $0 < n_a < 1$ and around $n_a^c = 1/2$, that is, $-1/2 < \delta < 1/2$, and $|\delta|$ is very small. Using first-order perturbation theory, the generalized second-order coherence function in Eq. (45) is approximately

$$g^{(2)}(\tau, 0) \simeq \frac{X}{(j+1)jY}, \quad (48)$$

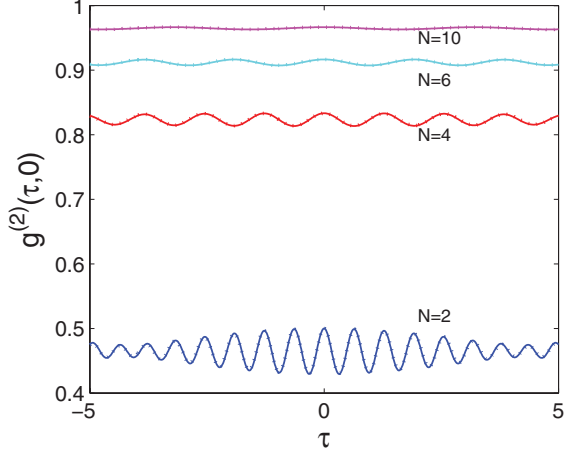


FIG. 5. (Color online) Second-order correlation function $g^{(2)}(\tau, 0)$ versus the time interval τ for $N = 2$ (blue curve), $N = 4$ (red curve), $N = 6$ (cyan curve), and $N = 10$ (magenta curve), respectively, in the case without dissipation. Recall that $g^{(2)}(\tau, 0)$ is proportional to the joint probability of observing one excited atom at time $t = 0$ and another one at time τ . The first-order approximate results are shown using dashed curves and the exact numerical results are shown using solid curves. The dashed curves overlap with the solid curves very well. Other parameters are $g_0 = 100$, $g_0/\Delta = -0.1$, $\Omega N = 0.1|W|$, $\delta = -0.02$.

where

$$\begin{aligned} X &\equiv x_1 + x_2 + x_3 + x_4 + x_5, \\ Y &\equiv y_1 + y_2 + y_3. \end{aligned} \quad (49)$$

The parameters x_{ℓ_1} ($\ell_1 = 1, 2, \dots, 5$) and y_{ℓ_2} ($\ell_2 = 1, 2, 3$) have complicated expressions, which are presented in the appendix. The generalized second-order coherence function given by Eq. (48) is illustrated in Fig. 5. It is shown that, as N increases, the value of $g^{(2)}(\tau, 0)$ approaches unity with some oscillations. Physically, Eq. (48) describes the joint probability of observing one excited atom at instant $t = 0$ and another after a time interval τ . In Sec. V, we use Eq. (48) to analyze the atomic blockade effect.

B. The case with dissipation

In this subsection, we consider the system surrounded by a thermal reservoir at zero temperature. When the system is prepared in a state with density operator ρ_s , the generalized second-order coherence function is written explicitly as

$$g^{(2)}(\tau, t) = \frac{\text{Tr}[J_+ J_+(\tau) J_-(\tau) J_- \rho_s(t)]}{\text{Tr}[J_+ J_- \rho_s(t)] \text{Tr}[J_+ J_- \rho_s(t + \tau)]}. \quad (50)$$

According to Eq. (50), we need to calculate the time-dependent density operator $\rho_s(t)$ of the atoms. In the regime of weak coupling of the driving field [53], which demands the driving field to only perturbatively change the energy levels, and assuming the atomic ensemble to be in a common reservoir, then the master equation is approximately

$$\frac{d\rho_s(t)}{dt} = -i[H^{(R)}, \rho_s(t)] + \gamma \left[J_- \rho_s(t) J_+ - \frac{1}{2} \{J_+ J_-, \rho_s(t)\} \right], \quad (51)$$

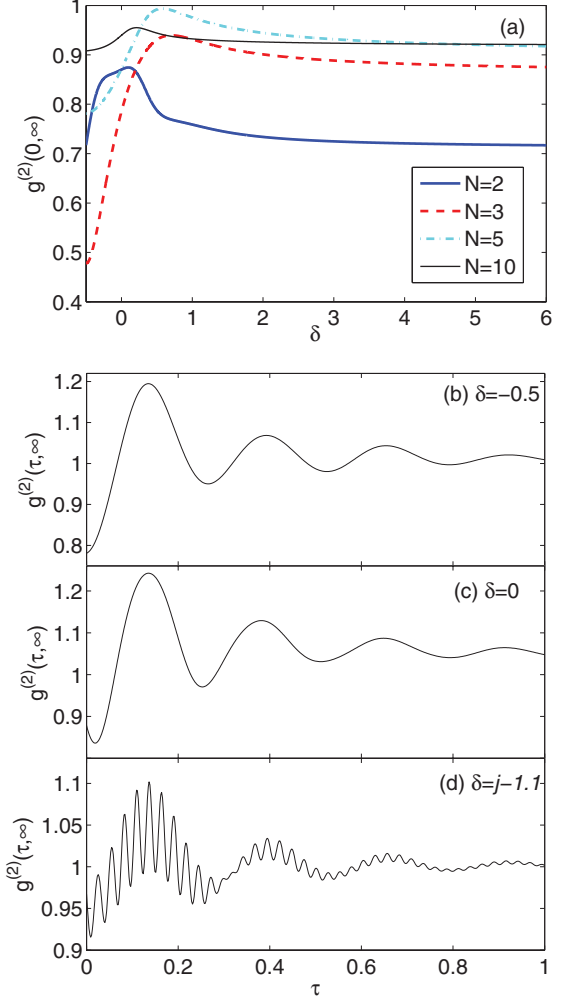


FIG. 6. (Color online) Numerical results for the generalized second-order coherence function $g^{(2)}(0, \infty)$ and $g^{(2)}(\tau, \infty)$ with dissipation in the steady state. (a) $g^{(2)}(0, \infty)$ versus δ for $N = 2$ (blue thick solid curve), $N = 3$ (red dashed curve), $N = 5$ (cyan dashed-dotted curve), and $N = 10$ (black thin solid curve), respectively; (b)–(d) $g^{(2)}(\tau, \infty)$ versus τ with $N = 5$ for $\delta = -0.5$, $\delta = 0$, and $\delta = j - 1.1$, respectively. Other common parameters are $\gamma = 1$, $g_0 = 100$, $g_0/\Delta = -0.1$, and $\Omega N = 0.1|W|$.

where γ is the collective decay rate of the atomic ensemble. Since the photon number is a conserved number, and the frequency of photons is in large detuning, it does not influence the dynamical evolution of the atoms. Then the influence of the decay of the photons is negligibly small to the atoms. We resort to numerical calculations to show the results about the steady state by plotting $g^{(2)}(0, t \rightarrow \infty)$ versus δ in Fig. 6(a) and $g^{(2)}(\tau, t \rightarrow \infty)$ versus τ in Figs. 6(b)–6(d). By comparing them with the results in Fig. 5, we will discuss them in the next section.

V. DOUBLE EXCITATION EFFECTS I: THE ATOMIC BLOCKADE EFFECT

In this and the next section, we discuss some physical effects due to the double collective excitation, according to their quantum statistics characterized by the generalized

second-order coherence function $g^{(2)}(\tau, t)$ introduced in the last section. We have calculated the generalized second-order coherence function in the above section both in the dissipation-free case and also the case with dissipation. In this section, we discuss the results in both cases according to the above calculations. We illustrate the analytical results (48) and compare them with the numerical results by plotting in Fig. 5 the generalized second-order coherence function $g^{(2)}(\tau, 0)$ versus the time interval τ around $\delta_c = 0$, without dissipation. The generalized second-order coherence function is plotted for $N = 2, 4, 6, 10$ atoms, respectively. It is clear from Fig. 5 that, close to the critical point $\delta_c = 0$, our analytical approximate results (48) (dashed line) agree very well with the numerical result (43) (solid line). Obviously, $g^{(2)}(\tau, 0) < 1$ at any time interval τ . This shows that the atomic collective symmetric excitations obey sub-Poissonian statistics. It can also be found that as N increases, $g^{(2)}(\tau, 0) < 1$ oscillates slower and slower and approaches unity, especially for $g^{(2)}(0, 0)$. That is because the generalized second-order coherence function at $\tau = 0$ is

$$g^{(2)}(0, 0) = 1 - \frac{4}{N^2 + 2N}. \quad (52)$$

Hence $g^{(2)}(0, 0)$ increases as N increases. In the thermodynamic limit $N \rightarrow \infty$,

$$g^{(2)}(0, 0) \rightarrow 1. \quad (53)$$

This shows that when N is smaller, the effect of suppressing the doubly excited state is enhanced.

Figure 6 shows the results for the dissipative case. Figure 6(a) shows $g^{(2)}(0, \infty)$ versus the average photon number δ in steady state for $N = 2, 3, 5, 10$ atoms, respectively. As shown in this figure, the value of $g^{(2)}(0, \infty)$ increases as N increases for a larger average photon number. For a definite N and a small value of δ , $g^{(2)}(0, \infty)$ increases as δ increases. At some intermediate time there is a peak in $g^{(2)}(0, \infty)$ followed by a steady decrease, asymptotically approaching a constant value for large δ . The smallest value of $g^{(2)}(0, \infty)$ occurs at $\delta = -0.5$. This phenomenon is also prominent in Figs. 6(b)–6(d). Figures 6(b)–6(d) show $g^{(2)}(\tau, \infty)$ versus τ for $N = 5$ and $\delta = -0.5, 0$ and $j = 1.1$, respectively. The antibunching effect of collective excitations of an atomic ensemble is observed since the envelop of $g^{(2)}(\tau, \infty)$ shows $g^{(2)}(0, \infty) < g^{(2)}(\tau, \infty)$ with some increasingly rapid oscillations as δ increases in Figs. 6(b)–6(d). Additionally we note that $g^{(2)}(\tau, \infty)$ approaches one, as expected, after some oscillations. This indicates the probability of two collective excitations of the atomic ensemble at the same time ($\tau = 0$) is smaller than that at a different time ($\tau \neq 0$). Therefore, the resonant excitations from the ground state to the doubly excited state are suppressed. This is a clear signature of the atomic blockade. Compared with Fig. 5, this result is better and closer to physical reality. As shown in Fig. 5, the generalized second-order coherence function only oscillates with time interval τ and does not approach 1 as we expect when $\tau \rightarrow \infty$. In Ref. [54], the photon antibunching effect is also obtained in only two interacting atoms. However, the antibunching effect we obtain is about atomic collective excitations, and the photon number is a conserved number. In this sense, we do not need to consider the photon correlation.

To conclude this section, we give some remarks about the atomic blockade. For applications in quantum information, the atomic blockade provides a novel approach to physical implementation of scalable quantum logic gates such as implementing a CNOT gate between two atoms [11–13] and some kinds of quantum protocols [55–58]. Furthermore, as double excitation are inhibited in the Rydberg blockade mechanism, it also supplies a fascinating approach to store quantum information [11, 12]. However, the dipole-dipole interaction depends on the distance between Rydberg atoms. To achieve a stronger interaction, it requires the atoms to be closer in space or to be excited to higher Rydberg states, in which the principal quantum number is very large, but this will not be convenient to control the atoms individually [11–13]. Such as the Rydberg levels $n = 79$ and 90 , the corresponding blockade shift is $2\pi \times 3$ and $2\pi \times 9.5$ MHz at an interatom distance $10.2 \mu\text{m}$, respectively. To achieve a larger energy-level shift due to the Rydberg blockade, the distance needs to be decreased, and thus the coherent manipulation of individual atoms is difficult. It is this consideration that motivates us to find a new mechanism inducing a stronger interatom coupling, valid for long distances and controllable to improve the dipole-dipole interaction. We note that in Ref. [59], the coupling strength between atom and photons can reach $2\pi \times 120$ MHz in a high-finesse cavity, which leads us to anticipate that the strong atom-photon coupling will induce a stronger interatom interaction among atoms. In addition, this interaction can be feasibly controlled by the volume of high-finesse microcavities. This fact means that to achieve a strong interatom interaction among atoms will not take stringent requirements on manipulating atoms individually. Therefore, from the point of view of the controllability and strength of the interaction, the photon-induced interaction among atoms in our system is better than the dipole-dipole interaction inducing the Rydberg blockade.

VI. DOUBLE EXCITATION EFFECTS II: SENSITIVITY OF THE QUANTUM PHASE TRANSITION

As the system possesses QPTs, we now analyze how to control the QPT by photons in the cavity. To show the effect of the QPT on $g^{(2)}(\tau, 0)$ more clearly, we consider the $g^{(2)}(\tau, 0)$ around the critical point $n_a^c = j - 1/2$ at a fixed time interval τ . Then, according to Eq. (44) we choose $c_{j-1} = c_j = 1/\sqrt{2}$ and $c_m = 0$ ($m \neq j - 1, j$) in the initial state, namely

$$|\psi^c(0)\rangle = \frac{1}{\sqrt{2}}|j, j-1\rangle + \frac{1}{\sqrt{2}}|j, j\rangle. \quad (54)$$

With the relations $U(\tau) = U_0^c(\tau)U_I^c(\tau)$ for $U_0^c(\tau) = \exp(iH_0^c\tau)$, $U_I^c(\tau) = T \exp[-i \int_0^\tau V_I^c(\tau')d\tau']$, it follows from Eq. (43) that

$$\begin{aligned} U_0^{c\dagger}(\tau)J_+J_-U_0^c(\tau) &= i\alpha(t)(|j, j-1\rangle\langle j, j| - |j, j\rangle\langle j, j-1|) \\ &\quad + \beta(t)(|j, j-1\rangle\langle j, j| + |j, j\rangle\langle j, j-1|) \\ &\quad + \gamma(t)(|j, j\rangle\langle j, j| - |j, j-1\rangle\langle j, j-1|) \\ &\quad + J_+J_-. \end{aligned} \quad (55)$$

The explicit expressions of the coefficients $\alpha(t)$, $\beta(t)$ and $\gamma(t)$ are given in the Appendix.

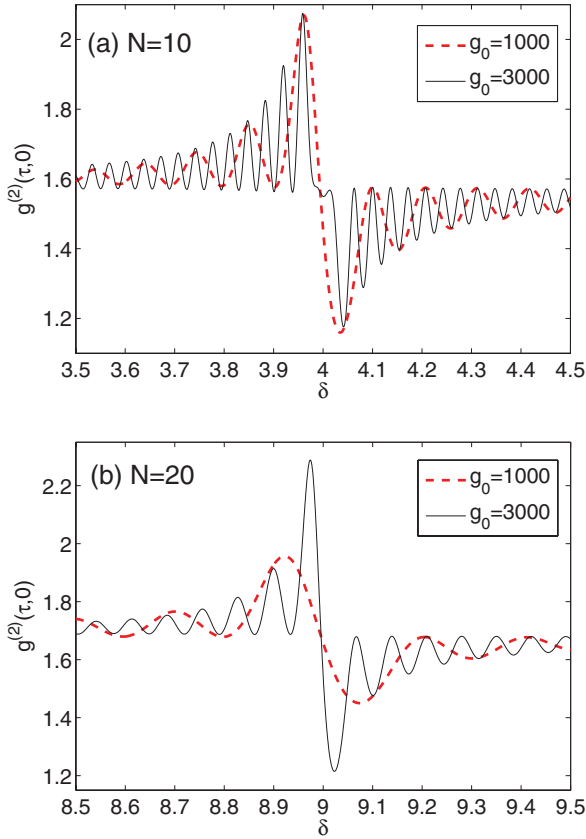


FIG. 7. (Color online) Numerical results for the generalized second-order coherence function $g^{(2)}(\tau, 0)$. Here $t = 0$, $\tau = 3$, $g_0 = 1000$ (red thick solid curve), $g_0 = 3000$ (black thin solid curve), (a) $N = 10$, $\delta_c = 4$, (b) $N = 20$, $\delta_c = 9$; other parameters are the same as in Fig. 5.

Next, we use the perturbation approach to calculate the generalized second-order coherence function under the following conditions for $m' = j - 2$, $r = 0, 1$, and $m \neq j - 2, j - 1, j$,

$$\Omega_{j-1}\eta_3^c \ll \Delta_{j-2,0}^c, \quad \Omega_{j-1}\eta_4^c \ll \Delta_{j-2,1}^c, \quad \Omega_{m+1} \ll \omega_{m+1,m}. \quad (56)$$

Up to first order in $V_I^c(\tau)$, we obtain

$$g^{(2)}(\tau, 0) \simeq \frac{\sum_{\ell_1=1}^7 x_{\ell_1}^c}{(3j-1)(\sum_{\ell_2=1}^4 y_{\ell_2}^c)}, \quad (57)$$

where the parameters $x_{\ell_1}^c$ ($\ell_1 = 1, 2, \dots, 7$) and $y_{\ell_2}^c$ ($\ell_2 = 1, 2, 3, 4$) have very long expressions, so we give these in the Appendix.

We also numerically calculate the generalized second-order coherence function in Eq. (43), and then plot $g^{(2)}(\tau, 0)$ versus δ in Fig. 7. As Fig. 7 indicates, the statistical coherence of atomic excitations is very sensitive to the critical point $n_a^c = j - 1/2$. The probability of double atomic excitation is above the dotted straight line in the left-hand side of the critical point, while it is below this curve in the right-hand side of the critical point. Furthermore the envelope exponentially decays. When the average photon number is in the domain of $j - 1 \leq n_a \leq j - 1/2$ ($j - 3/2 \leq \delta \leq j - 1$), the energy level of $|j, j\rangle$ is higher than $|j, j - 1\rangle$ but lower than $|j, j - 2\rangle$; while in the domain of $[j - 1/2, j]$, the energy level of $|j, j\rangle$ is lower than

both $|j, j - 1\rangle$ and $|j, j - 2\rangle$, and the order of the energy levels is $\omega_j < \omega_{j-1} < \omega_{j-2} < \dots < \omega_{-j}$. We also note that, as the coupling strength g_0 increases, $g^{(2)}(\tau, 0)$ oscillates faster with respect to δ . In addition, as N increases, the value of $g^{(2)}(\tau, 0)$ increases.

Above, we gave a qualitative analysis of the generalized second-order coherence function based on perturbation theory. According to our calculations, there is a large discrepancy between the theoretical analysis and the exact numerical result. The reason may be as follows. As seen in the definition of the generalized second-order coherence function [i.e., Eq. (43)], this is determined by two correlation functions, that is, $\langle \psi'(\tau) | U_I^{\dagger c}(\tau) J_+ J_- U_I^c(\tau) | \psi'(0) \rangle$ and $\langle \psi(0) | U_I^{\dagger c}(\tau) J_+ J_- U_I^c(\tau) | \psi(0) \rangle$. As far as the latter is concerned, we calculate it in the interaction picture. Here, we approximate the time-dependent wave function $U_I^c(\tau) | \psi(0) \rangle$ to first-order by perturbation theory. Since the operator $J_+ J_-$ gives two large and markedly different eigenvalues to the components $|j, j\rangle$ and $|j, j - 1\rangle$, the originally small deviation in the approximate wave function with respect to the exact one will be enlarged.

However, when we come to the case with $m = 0$ and 1, the situation turns out to be totally different. First of all, let us turn to the Hamiltonian $H = H_0 + H_I$ given in Eqs. (17) and (8). In the large-detuning regime, it only induces a Rabi oscillation between the two nearly degenerate states $|j, 0\rangle$ and $|j, 1\rangle$, while leaving the populations in the other states almost unchanged. On account of the conservation of the total probability and the same eigenvalues of the operator $J_+ J_-$ on the two relevant states, in the system which is initially in an equal superposition of $|j, 0\rangle$ and $|j, 1\rangle$, the approximate correlation function $\langle \psi(0) | U_I^{\dagger c}(\tau) J_+ J_- U_I^c(\tau) | \psi(0) \rangle$ is expected to be quite close to the exact one. This situation will not take place for the case with $m = j$ and $j - 1$, since the relevant eigenvalues of the operator $J_+ J_-$ are remarkably different from each other. A similar analysis can be applied to the numerator in the generalized second-order coherence function. Consequently, the generalized second-order coherence function obtained from the perturbation theory will coincide with the exact one for the case with $m = 0$ and 1, while there is an obvious difference between the results from these two methods for the case with $m = j$ and $j - 1$. Therefore, we only give the numerical results in Fig. 7.

VII. CONCLUSION AND REMARKS

In this paper, we study the statistical properties of atomic excitations for two cases: with dissipation and without dissipation. We find that this statistical property can be controlled by the average photon number in the cavity. In addition, the photon-induced second-order interaction between atoms is valid in the long range and can be strengthened by a high-finesse microcavity with a very small effective mode volume. Furthermore, we find that the double atomic excitation will be suppressed when the average photon number in the cavity is in the vicinity of some special points (degenerate points). We have also studied the critical behavior of this statistical property of atomic excitations around the critical point at which the QPT occurs.

To characterize the statistical property of atomic excitations, we define a generalized second-order coherence function similar to the second-order coherence function for photons. Furthermore, in the limit of $N \rightarrow \infty$ and low excitations, it becomes the conventional one. We have demonstrated the antibunching effect for atomic excitations near the degenerate points and the characteristic of sub-Poissonian statistics, which implies the existence of the atomic excitation blockade. Since this system possesses several critical points, we also study the critical behavior of the generalized second-order coherence function of atomic excitations around the critical points. Our results show the sensitivity of the system dynamics with the average photon number in the cavity.

ACKNOWLEDGMENTS

We thank J.-N. Zhang and Chengyun Cai for helpful discussions in numerical calculations, and M. Delanty and A. Miranowicz for helpful discussions and very useful suggestions on the manuscript. The work is supported by the National Natural Science Foundation of China under Grants No. 10935010 and No. 11074261. F.N. acknowledges partial support from the Laboratory of Physical Sciences, National Security Agency, Army Research Office, National Science Foundation Grant No. 0726909, Grant-in-Aid for Scientific Research (S), MEXT Kakenhi on Quantum Cybernetics, and the JSPS-FIRST program.

APPENDIX: EXPLICIT EXPRESSIONS FOR THE PARAMETERS OF $g^{(2)}$

In this Appendix, we present the expressions for the parameters used in Eqs. (48) and (57), respectively.

For $m = 0, 1$, the parameters of $g^{(2)}(\tau, 0)$ given by Eq. (48) are

$$\begin{aligned} x_1 &= v_0^2(j-1)^2(j+2)^2|c_1|^2|\eta_1\eta_3O_{2,0} + \eta_2\eta_4O_{2,1}|^2, \\ x_2 &= v_0^2(j+1)^2j^2|c_0|^2\left(\frac{\eta_3\eta_4}{\eta_2\eta_3 - \eta_1\eta_4}\right)^2|O_{-1,0}^* - O_{-1,1}^*|^2, \\ x_3 &= j^2(j+1)^2\left|\frac{v_0c_0(\eta_4\eta_1O_{-1,1}^* - \eta_3\eta_2O_{-1,0}^*)}{\eta_2\eta_3 - \eta_1\eta_4} + c_1\right|^2, \\ x_4 &= j(j+2)(j^2-1)|v_0c_1(\eta_3^2O_{-1,0} + \eta_4^2O_{-1,1}) + c_0|^2, \\ x_5 &= v_0^2(j-1)(j^2-4)(j+3)\frac{|c_0|^2}{\omega_{-2,-1}^2}|1 - e^{i\omega_{-2,-1}\tau}|^2, \end{aligned} \quad (\text{A1})$$

and

$$\begin{aligned} y_1 &= (j+1)j, \\ y_2 &= \Omega^2(j-1)^2(j+2)^2|\eta_1(c_0\eta_3 + c_1\eta_1)O_{2,0} \\ &\quad + \eta_2(c_0\eta_4 + c_1\eta_2)O_{2,1}|^2, \end{aligned}$$

$$\begin{aligned} y_3 &= v_0^2(j-1)(j+2)|\eta_3(c_0\eta_3 + c_1\eta_1)O_{-1,0} \\ &\quad + \eta_4(c_0\eta_4 + c_1\eta_2)O_{-1,1}|^2, \end{aligned} \quad (\text{A2})$$

where

$$v_0 \equiv \Omega\sqrt{(j+1)j}, \quad O_{m,n} \equiv \frac{1}{\Delta_{m,n}}(1 - e^{i\Delta_{m,n}\tau}). \quad (\text{A3})$$

For $m = j-1, j$, the parameters of $g^{(2)}(\tau, 0)$ given by Eq. (57) are listed as follows:

$$\begin{aligned} x_1^c &= 2j|a_0(\tau)|^2, \\ x_2^c &= 2(2j-1)|a_1(\tau)|^2, \\ x_3^c &= 3(2j-2)|a_2(\tau)|^2, \\ x_4^c &= 4(2j-3)|a_3(\tau)|^2, \\ x_5^c &= -2\alpha(\tau)\text{Im}[a_0(\tau)a_1^*(\tau)], \\ x_6^c &= 2\beta(\tau)\text{Re}[a_0(\tau)a_1^*(\tau)], \\ x_7^c &= \gamma(\tau)[|a_0(\tau)|^2 - |a_1(\tau)|^2], \end{aligned} \quad (\text{A4})$$

and

$$\begin{aligned} y_1^c &= j, \quad y_2^c = 2j-1, \\ y_3^c &= 3(2j-2)|c_2|^2, \quad y_4^c = \beta(\tau), \end{aligned} \quad (\text{A5})$$

where

$$\begin{aligned} a_0(\tau) &= \eta_3^c\eta_4^cf^c(O_{j-2,0}^{c*} - O_{j-2,1}^{c*}), \\ a_1(\tau) &= \sqrt{j} - f^c(\eta_2^c\eta_3^cO_{j-2,0}^{c*} - \eta_1^c\eta_4^cO_{j-2,1}^{c*}), \\ a_2(\tau) &= \sqrt{2j-1}\left[1 + \frac{f^c\sqrt{j}}{2j-1}h_1(\tau)\right], \\ a_3(\tau) &= \Omega\sqrt{3(2j-1)(2j-2)}\frac{(1 - e^{i\omega_{j-3,j-2}\tau})}{\omega_{j-3,j-2}}, \\ c_2(\tau) &= \frac{f^ch_2(\tau)}{\sqrt{2(2j-1)}}, \end{aligned} \quad (\text{A6})$$

and

$$\begin{aligned} \alpha(t) &= q_0q^{-1}\sin(qt), \\ \beta(t) &= q_0q^{-2}(\omega_{j-1} - \omega_j)[\cos(qt) - 1], \\ \gamma(t) &= 2q_0q^{-2}\Omega\sqrt{2j}[\cos(qt) - 1], \end{aligned} \quad (\text{A7})$$

with

$$\begin{aligned} q_0 &\equiv -2\Omega\sqrt{2j(j-1)}, \quad f^c \equiv \frac{\sqrt{2}\Omega(2j-1)}{\eta_2^c\eta_3^c - \eta_1^c\eta_4^c}, \\ q &\equiv \sqrt{(\omega_{j-1} - \omega_j)^2 + 8j\Omega^2}, \quad O_{m,n}^c \equiv \frac{1 - e^{i\Delta_{m,n}^c\tau}}{\Delta_{m,n}^c}. \end{aligned} \quad (\text{A8})$$

Here,

$$\begin{aligned} h_1(\tau) &= \eta_2^c\eta_3^cO_{j-2,0}^c - \eta_1^c\eta_4^cO_{j-2,1}^c, \\ h_2(\tau) &= \eta_3^c(\eta_2^c - \eta_4^c)O_{j-2,0}^c - \eta_4^c(\eta_1^c - \eta_3^c)O_{j-2,1}^c. \end{aligned} \quad (\text{A9})$$

- [1] R. J. Glauber, *Phys. Rev. Lett.* **10**, 84 (1963); *Phys. Rev.* **130**, 2529 (1963).
 [2] D. F. Walls and G. J. Milburn, *Quantum Optics* (Springer-Verlag, Berlin, 1994).

- [3] A. Imamoglu, H. Schmidt, G. Woods, and M. Deutsch, *Phys. Rev. Lett.* **79**, 1467 (1997).
 [4] K. M. Birnbaum, A. Boca, R. Miller, A. D. Boozer, T. E. Northup, and H. J. Kimble, *Nature (London)* **436**, 87 (2005).

- [5] W. Leoński and A. Miranowicz, *Adv. Chem. Phys.* **119**, 195 (2001); A. Miranowicz, W. Leoński, and N. Imoto, *ibid.* **119**, 155 (2001).
- [6] N. Lambert, Y.-N. Chen, and F. Nori, *Phys. Rev. A* **82**, 063840 (2010).
- [7] D. Meiser and P. Meystre, *Phys. Rev. Lett.* **94**, 093001 (2005).
- [8] D. F. Phillips, A. Fleischhauer, A. Mair, R. L. Walsworth, and M. D. Lukin, *Phys. Rev. Lett.* **86**, 783 (2001); M. D. Lukin, *Rev. Mod. Phys.* **75**, 457 (2003).
- [9] C. P. Sun, Y. Li, and X. F. Liu, *Phys. Rev. Lett.* **91**, 147903 (2003); C. P. Sun, S. Yi, and L. You, *Phys. Rev. A* **67**, 063815 (2003).
- [10] G. R. Jin, P. Zhang, Y. X. Liu, and C. P. Sun, *Phys. Rev. B* **68**, 134301 (2003).
- [11] M. D. Lukin, M. Fleischhauer, R. Cote, L. M. Duan, D. Jaksch, J. I. Cirac, and P. Zoller, *Phys. Rev. Lett.* **87**, 037901 (2001).
- [12] E. Urban, T. A. Johnson, T. Henage, L. Isenhower, D. D. Yavuz, T. G. Walker, and M. Saffman, *Nature Phys.* **5**, 110 (2009).
- [13] A. Gaëtan, Y. Miroshnychenko, T. Wilk, A. Chotia, M. Viteau, D. Comparat, P. Pillet, A. Browaeys, and P. Grangier, *Nature Phys.* **5**, 115 (2009).
- [14] D. V. Averin and K. K. Likharev, *J. Low Temp. Phys.* **62**, 345 (1986).
- [15] T. A. Fulton and G. J. Dolan, *Phys. Rev. Lett.* **59**, 109 (1987).
- [16] K. Ono, D. G. Austing, Y. Tokura, and S. Tarucha, *Science* **297**, 1313 (2002).
- [17] M. A. Kastner, *Rev. Mod. Phys.* **64**, 849 (1992); *Phys. Today* **46**, 24 (1993).
- [18] N. Schlosser, G. Reymond, I. Protchenko, and P. Grangier, *Nature (London)* **411**, 1024 (2001).
- [19] Y. X. Liu, A. Miranowicz, Y. B. Gao, J. Bajer, C. P. Sun, and F. Nori, *Phys. Rev. A* **82**, 032101 (2010).
- [20] N. Lütkenhaus, *Phys. Rev. A* **61**, 052304 (2000).
- [21] J. Ma, X. Wang, C. P. Sun, and F. Nori, *Phys. Rep.* **509**, 89 (2011).
- [22] S. Sachdev, *Quantum Phase Transitions* (Cambridge University Press, Cambridge, 1999).
- [23] X. F. Shi, Y. Yu, J. Q. You, and F. Nori, *Phys. Rev. B* **79**, 134431 (2009).
- [24] J. Q. You, X. F. Shi, X. Hu, and F. Nori, *Phys. Rev. B* **81**, 014505 (2010).
- [25] H. J. Lipkin, N. Meshkov, and A. J. Glick, *Nucl. Phys.* **62**, 188 (1965); N. Meshkov, A. J. Glick, and H. J. Lipkin, *ibid.* **62**, 199 (1965); A. J. Glick, H. J. Lipkin, and N. Meshkov, *ibid.* **62**, 211 (1965).
- [26] A. Miranowicz, Ş. K. Özdemir, Y. X. Liu, M. Koashi, N. Imoto, and Y. Hirayama, *Phys. Rev. A* **65**, 062321 (2002).
- [27] H. T. Quan, Z. Song, X. F. Liu, P. Zanardi, and C. P. Sun, *Phys. Rev. Lett.* **96**, 140604 (2006).
- [28] H. T. Quan, Z. D. Wang, and C. P. Sun, *Phys. Rev. A* **76**, 012104 (2007).
- [29] J. F. Huang, Y. Li, J. Q. Liao, L. M. Kuang, and C. P. Sun, *Phys. Rev. A* **80**, 063829 (2009).
- [30] Q. Ai, Y. D. Wang, G. L. Long, and C. P. Sun, *Sci. China Ser G* **52**, 1898 (2009).
- [31] C. Emary and T. Brandes, *Phys. Rev. Lett.* **90**, 044101 (2003); *Phys. Rev. E* **67**, 066203 (2003).
- [32] R. H. Dicke, *Phys. Rev.* **93**, 99 (1954).
- [33] Y. Kaluzny, P. Goy, M. Gross, J. M. Raimond, and S. Haroche, *Phys. Rev. Lett.* **51**, 1175 (1983).
- [34] F. Brennecke, T. Donner, S. Ritter, T. Bourdel, M. Kohl, and T. Esslinger, *Nature (London)* **450**, 268 (2007).
- [35] M. Delanty, S. Rebic, and J. Twamley, *New J. Phys.* **13**, 053032 (2011).
- [36] Y. Li, Z. D. Wang, and C. P. Sun, *Phys. Rev. A* **74**, 023815 (2006).
- [37] Y. Li, P. Zhang, and Z. D. Wang, *Eur. Phys. J. D* **58**, 379 (2010).
- [38] N. Lambert, Y. N. Chen, R. Johannsson, and F. Nori, *Phys. Rev. B* **80**, 165308 (2009).
- [39] F. Dimer, B. Estienne, A. S. Parkins, and H. J. Carmichael, *Phys. Rev. A* **75**, 013804 (2007).
- [40] D. Nagy, G. Kónya, G. Szirmai, and P. Domokos, *Phys. Rev. Lett.* **104**, 130401 (2010).
- [41] K. Rzazewski, K. Wódkiewicz, and W. Zacobowicz, *Phys. Rev. Lett.* **35**, 432 (1975).
- [42] I. Bialynicki-Birula and K. Rzazewski, *Phys. Rev. A* **19**, 301 (1979).
- [43] P. Nataf and C. Ciuti, *Nat. Commun.* **1**, 72 (2010).
- [44] H. Fröhlich, *Phys. Rev.* **79**, 845 (1950); *Proc. R. Soc. London A* **215**, 291 (1952); *Adv. Phys.* **3**, 325 (1954).
- [45] S. Nakajima, *Adv. Phys.* **4**, 363 (1955).
- [46] C. P. Sun, Y. X. Liu, L. F. Wei, and F. Nori, e-print arXiv:quant-ph/0506011.
- [47] D. I. Tsomokos, S. Ashhab, and F. Nori, *New J. Phys.* **10**, 113020 (2008).
- [48] J. Larson, *Europhys. Lett.* **90**, 54001 (2010).
- [49] S. Dusuel and J. Vidal, *Phys. Rev. B* **71**, 224420 (2005).
- [50] J. I. Latorre, R. Orus, E. Rico, and J. Vidal, *Phys. Rev. A* **71**, 064101 (2005).
- [51] J. Q. You, Y. X. Liu, C. P. Sun, and F. Nori, *Phys. Rev. B* **75**, 104516 (2007); J. Q. You, Y. X. Liu, and F. Nori, *Phys. Rev. Lett.* **100**, 047001 (2008); H. Ian, Y. X. Liu, and F. Nori, *Phys. Rev. A* **81**, 063823 (2010).
- [52] T. Holstein and H. Primakoff, *Phys. Rev.* **58**, 1098 (1940).
- [53] H. P. Breuer and F. Petruccione, *The Theory of Open Quantum Systems* (Oxford University Press, Oxford, 2002).
- [54] Z. Ficek, R. Tanaś, and S. Kielich, *Phys. Rev. A* **29**, 2004 (1984).
- [55] M. Saffman and T. G. Walker, *Phys. Rev. A* **66**, 065403 (2002).
- [56] M. Saffman and T. G. Walker, *Phys. Rev. A* **72**, 042302 (2005).
- [57] E. Brion, K. Mølmer, and M. Saffman, *Phys. Rev. Lett.* **99**, 260501 (2007).
- [58] E. Brion, A. S. Mouritzen, and K. Mølmer, *Phys. Rev. A* **76**, 022334 (2007).
- [59] C. J. Hood, M. S. Chapman, T. W. Lynn, and H. J. Kimble, *Phys. Rev. Lett.* **80**, 4157 (1998).